TÜBİTAK

Turkish Journal of Engineering & Environmental Sciences

http://journals.tubitak.gov.tr/engineering/

Research Article

Turkish J Eng Env Sci
(2014) 38: 278 – 292

doi:10.3906/muh-1208-6

Boundary shear stress in asymmetric rectangular compound channels

Issam A. AL-KHATIB[1*], **Mustafa GÖĞÜŞ**[2]

[1]Institute of Environmental and Water Studies, Birzeit University, Birzeit, West Bank, Palestine

[2]Hydraulics Division, Civil Engineering Department, Middle East Technical University, Ankara, Turkey

Received: 13.08.2012 • **Accepted/Published Online:** 10.04.2015 • **Printed:** 30.06.2015

Abstract: A series of nine experiments was performed in a physical model of an asymmetric compound channel to quantify the boundary shear stress at the interface of the bed of a main channel and floodplain. Commonly used equations of shear stress distributions across the bottoms of the main channel and floodplain interfaces were analyzed and tested for various types of asymmetric compound channels and their flow conditions. The lateral momentum transfer between the deep main channel and the adjoining shallow floodplains was found to greatly affect the shear stress distribution at the bottoms of the main channel and the flood plain subsections. Different dimensionless ratios of shear stress distributions were obtained and related to the relevant parameters. Some important results concerning the uniformity of the shear stress distribution, which is significant in sediment-laden rivers to state the possible locations of erosion and deposition, are presented.

Key words: Open channel, asymmetric compound channel, momentum transfer, boundary shear, floodplain, main channel

1. Introduction

Water flowing in ducts and open channels exerts longitudinal shear stress on the wetted periphery that is not distributed uniformly. Distribution of the boundary shear stress depends upon the shape of the cross section, the structure of the secondary flow cells, and lack of uniformity in the boundary roughness. Boundary shear stress distribution is important in predicting flow resistance, sediment transport, and cavitation. It is essential for practicing river engineers to understand the shear stress distribution along the periphery of open channels for the prediction of river morphology as well as for the protection of the river bed, river banks, and flood control structures [1–5].

The determination of bed shear stress and side-wall shear stress is important in open channel flows studies. For example, many authors have determined boundary shear stress to study the velocity profile [6–8]. Separation of bed shear stress from total shear stress is important for estimating the bed load transport in open channel flows. Similarly, to study channel migration or to prevent bank erosion, one must know the side-wall shear stress. Moreover, the shear stress measurement is often needed in laboratory flume studies of bed form resistance and sediment transport [9–11]. Wall shear stress measurement techniques were recently reviewed by Bocchiola et al. [12]. Bed load transport comprises a series of random events associated with the motion of bed sediment particles. In describing the motion of the particles in the probabilistic approach, evaluations of the probability density functions of the hydrodynamic forces exerted on the particles are essential for conducting relevant analyses [13].

*Correspondence: ikhatib2012@yahoo.com

Bed shear stress can serve in characterizing the flow effect on the motion of bed particles. It has often been included in formulations of sediment transport, for example, those related to the critical condition for the initiation of sediment motion and bed load transport rates [13]. Many authors have studied uniform channel flows and boundary layers [14–18]. The measurements conducted in these studies show that the distribution of bed shear stress is always skewed. Cheng et al. [13] reported that the probability density distribution derived from experimental data could be represented well by the lognormal function, rather than the widely used Gaussian function. However, the experimental data collected in previous studies were usually limited to simple situations such as uniform open channel flows [19] and boundary layers [13,20]. Deformation of various kinds of river cross sections are related to scour or deposition that are directly related to boundary shear stress [21–24].

The boundary shear stress distribution and flow resistance in the cross section of compound channels have been investigated by many authors [25–33].

The aim of the present study was to describe the effect of the interaction mechanism on the shear stress distribution in an asymmetric channel of compound cross section. In particular, the effect of the main channel width and step height on the variation in shear stress distribution in both the main channel and floodplain channel was investigated.

2. Experimental apparatus and procedure

The experiments were carried out in a glass-walled horizontal laboratory flume 7.5 m long, 0.30 m wide, and 0.3 m deep with a bottom slope of 0.0025 at the fluid mechanics laboratory, Mechanical Engineering Department, Birzeit University, Palestine. Discharge was measured volumetrically with a flow meter with 0.1 L accuracy. A point gauge was used along the centerline of the flume for head measurements. All depth measurements were done with respect to the bottom of the flume. A pitot tube of circular section with external diameter of 8 mm was used to measure the static and total pressures, which were used for velocities and shear stresses at required points in the experiments conducted throughout this study.

The models of asymmetric rectangular compound cross sections were manufactured from Plexiglas and placed at about mid length of the laboratory flume. Figures 1a and 1b show the plan view and cross section of the models, respectively, with symbols designating important dimensions of the model elements. The dimensions of the various models used in the experiments are given in the Table. The model types tested in this study are denoted by BIZJ (I = 1, 2, 3; J = 1, 2, 3). Here B and Z are the width and step height of the main channel of the asymmetric compound cross section, respectively.

Table. Geometrical properties of the asymmetric rectangular compound channel models.

Models	B	Z	B_f	B_O	θ_1	θ_2	B_O/B_f	B_O/Z	B_O/B	B_f/Z	B_f/B	B/Z
	(cm)	(cm)	(cm)	(cm)	(degrees)	(degrees)	(-)	(-)	(-)	(-)	(-)	(-)
B1Z1	10	2	20	30	26.57	153.43	1.50	15.00	3.00	10.00	2.00	5.00
B1Z2	10	4	20	30	26.57	153.43	1.50	7.50	3.00	5.00	2.00	2.50
B1Z3	10	6	20	30	26.57	153.43	1.50	5.00	3.00	3.33	2.00	1.67
B2Z1	15	2	15	30	26.57	153.43	2.00	15.00	2.00	7.50	1.00	7.5
B2Z2	15	4	15	30	26.57	153.43	2.00	7.50	2.00	3.75	1.00	3.75
B2Z3	15	6	15	30	26.57	153.43	2.00	5.00	2.00	2.50	1.00	2.5
B3Z1	20	2	10	30	26.57	153.43	3.00	15.00	1.50	5.00	0.50	10.00
B3Z2	20	4	10	30	26.57	153.43	3.00	7.50	1.50	2.50	0.50	5.00
B3Z3	20	6	10	30	26.57	153.43	3.00	5.00	1.50	1.67	0.50	3.33

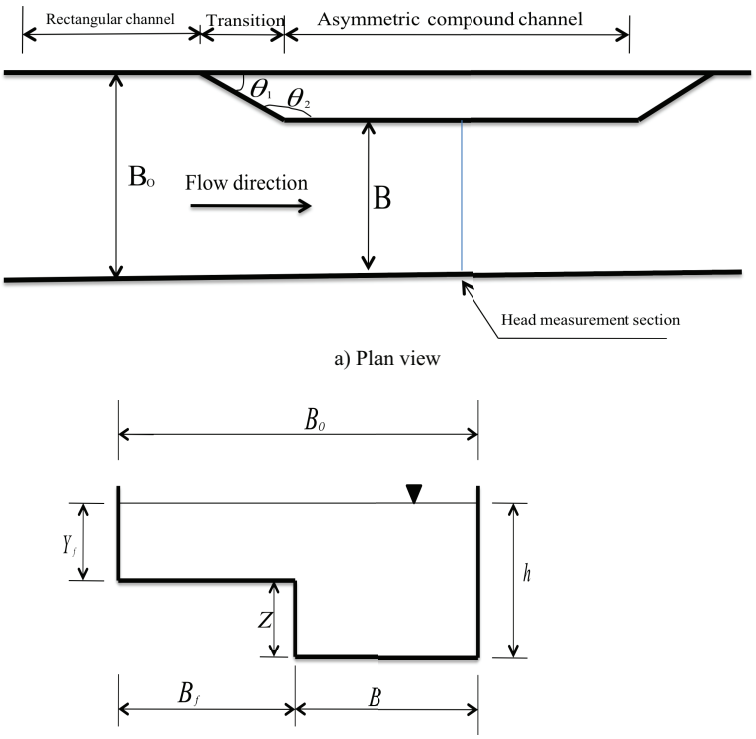

Figure 1. Definition sketch of the flume used in the experiments.

The required experiments first were conducted in the models of smallest B (=10 cm) with varying Z values (=2 cm, 4 cm, and 6 cm) and then B was increased to 15 cm at the required amount of Z (=2 cm, 4 cm, and 6 cm), and finally for B = 20 cm with the same three values of Z. The entrance angles, θ_1 and θ_2, were 26.565° and 153.35°, respectively. The transition length was twice the floodplain width, B_f, and the length of the asymmetrical rectangular compound channel section in all tested models was 2 m. From velocity measurements of the flows tested it was verified that the length of the channel was long enough to get fully developed flow.

2.1. Measurement of wall shear stress

Preston [34] developed a simple technique for measuring the local shear stress on smooth boundaries in a turbulent boundary layer using a pitot tube (or Preston tube) placed in contact with the surface. The method is based on the assumption of an inner law (law of the wall), which relates the boundary shear stress to the velocity distribution near the wall. Assessment of the near wall velocity distribution is empirically inferred from the differential pressure between the pitot tube and static wall pressure tapping. Patel [35] undertook further experiments to produce a reliable and definitive calibration curve to replace the one developed by Preston. Patel's calibration curve, which has been shown to be reliable, may be summarized as follows [36,37]:

$$X^* = log_{10}\left[\frac{\Delta P d^2}{4\rho\nu^2}\right] \tag{1}$$

and

$$Y^* = log_{10}\left[\frac{\tau_o d^2}{4\rho\nu^2}\right], \tag{2}$$

where ΔP = is the Preston tube pressure difference; d = probe outside diameter; ρ = fluid density; ν = kinematic viscosity of the fluid; τ_o = boundary shear stress; X^* = the log of the dimensionless differential pressure; Y^* = the log of the dimensionless shear stress. Patel [35] produced three equations covering the range 0.0 <Y* <5.3:

$$Y^* = 0.5X^* + 0.0373$$

$$T_1 \text{ or } T_2 = \frac{\sum\limits_k \Delta X_k . T_k}{\sum\limits_k \Delta X_k} \tag{3}$$

$Y^* = 0.8287 - 0.1381X^* + 0.1437X^{*2} - 0.0060X^{*3}$ 4

$$T_1 \, or \, T_2 = \frac{\sum\limits_k \Delta X_k . T_k}{\sum\limits_k \Delta X_k} \tag{4}$$

and

$$X^* = Y^* + 2log_{10}\left[1.95Y^* + 4.0\right] 5$$

$$T_1 \, or \, T_2 = \frac{\sum\limits_k \Delta X_k . T_k}{\sum\limits_k \Delta X_k} \tag{5}$$

where Eq. (3) is applicable for 0.0 < Y* < 1.5,

Eq. (4) is applicable for 1.5 < Y* < 3.5, and

Eq. (5) is applicable for 3.5 < Y* < 5.3.

As can be seen, the Preston-tube method of obtaining the wall shear stress is much simpler than the Clauser plot. In the Clauser chart method [38], the friction velocity is extrapolated from direct measurements of the free stream velocity *and* the mean velocity profile U(y), where y is the normal distance from the wall. The method is based on the assumption that the velocity profile follows a universal logarithmic form in the overlap region of the boundary layer [39].

The technique has been widely used for the measurement of the boundary shear stresses in both smooth and rough open channels. Many authors [31,37,40–44] have utilized this technique.

To determine the wall shear stress at the bottom of the main channel and along the floodplain bottom, the measurements were taken by the Preston tube at successive points. Following the analysis of the measured data and then using Eqs. (3)–(5), the shear stress distributions at the main channel bottom and floodplain bottom were calculated for each experiment.

3. Presentation and discussion of the results

Shear stress patterns were obtained for different depths of flow (h), each corresponding to a certain discharge value. All of these depths were within the full compound cross section depth. The following notations are used to define 6 different types of shear stresses that are obtained from the measurements at the corresponding point locations:

T_1 = average shear stress at the bottom of the main channel obtained by averaging the calculated shear stress values as measured at specified points along the main channel cross section.

T_2 = average shear stress at the bed of the floodplain obtained by averaging the calculated shear stress values as measured at specified points along the floodplain cross section.

T_3 = maximum shear stress at the bottom of the main channel obtained by selecting the maximum calculated shear stress as measured at specified points along the main channel cross section.

T_4 = maximum shear stress at the bed of the floodplains obtained by selecting the maximum calculated shear stress as measured at specified points along the floodplain cross section.

T_5 = mean shear stress at the bottom of the main channel and equal to $\gamma \mathrm{R}_{mc} \mathrm{S}_0$; $\mathrm{R}_{mc} = \mathrm{A}_{mc}/P_{mc}$; $\mathrm{A}_{mc} = \mathrm{Bh}$, $P_{mc} = \mathrm{h} + \mathrm{B} + \mathrm{Z}$; γ is the specific weight of the fluid; R_{mc} is the hydraulic radius of the main channel; A_{mc} is the area of the main channel; P_{mc} is the wetted perimeter of the main channel; S_o is the energy slope.

T_6 = mean shear stress at the bed of the floodplain and equal to $\gamma R_f S_{0;} R_f = A_f/P_f; A_f = B_f(h - Z); P_f = (h - Z) + B_f; R_f$ is the hydraulic radius of the floodplain; A_f is the area of the floodplain; P_f is the wetted perimeter of the floodplain.

The average shear stresses (T_1 and T_2) are calculated as weighted averages by assuming a step function with step width (ΔX_k). For interior points along the main channel and floodplains, the shear stress measured at the kth point (T_k) is assumed to be constant along a step width that is equal to half the distance between points ($k-1$) and (k + 1). For points located at the 2 ends of the main channel and floodplains, the measured shear stress is assumed to be constant along a step width that is equal to half the distance between the end point and the adjacent one located in the same channel (i.e. main channel or floodplain channel). The step width is obtained from the point spacings along the wetted perimeter of the channel bottom. Eq. (6) is used to calculate the average shear stress.

$$T_1 \, or \, T_2 = \frac{\sum\limits_k \Delta X_k . T_k}{\sum\limits_k \Delta X_k} \tag{6}$$

The following subsections give details of the effect of the interaction mechanism on shear stress distribution in models of different geometry.

3.1. Variation in T_1 with discharge, Q

The relationship between T_1 and Q for some of the models tested is shown in Figures 2–5. The wall shear stress was integrated numerically over the bottom of the main channel and an average value, T_1, was obtained for each set of the experiments and plotted against the discharge. It can be seen from all the related figures that, in general, the average shear stress at the bottom of the main channel increases as discharge increases. In order to see the effect of the main channel width, B, on the values of T_1 for constant step height, Z, Figures 2 and 3 were plotted. From these two figures it is clearly seen that for a given discharge as B increases T_1 increases also. Figures 4 and 5 are another form of the data representation for T_1 and Q to investigate the effect of step height, Z, on T_1 as a function of Q for models of constant main channel width. From these two figures, in general one can conclude that as the Z values increase in channels of constant main channel for a given discharge, T_1 values increase, but sometimes decrease.

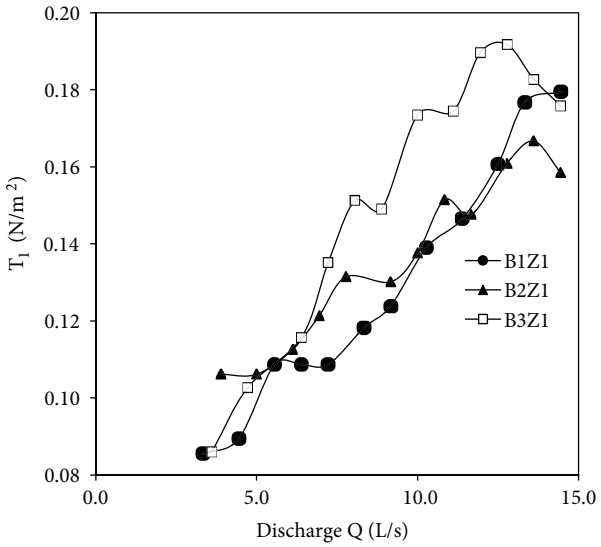

Figure 2. Average shear stress at the bottom of the main channel versus discharge for the models of constant step height (Z = 2 cm).

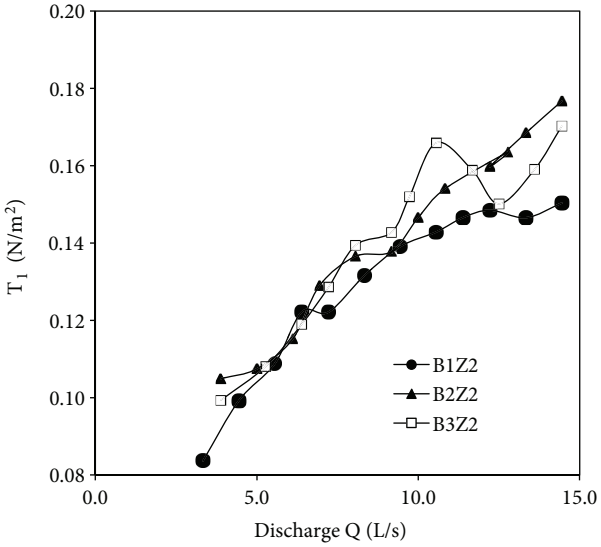

Figure 3. Average shear stress at the bottom of the main channel versus discharge for the models of constant step height (Z = 4 cm).

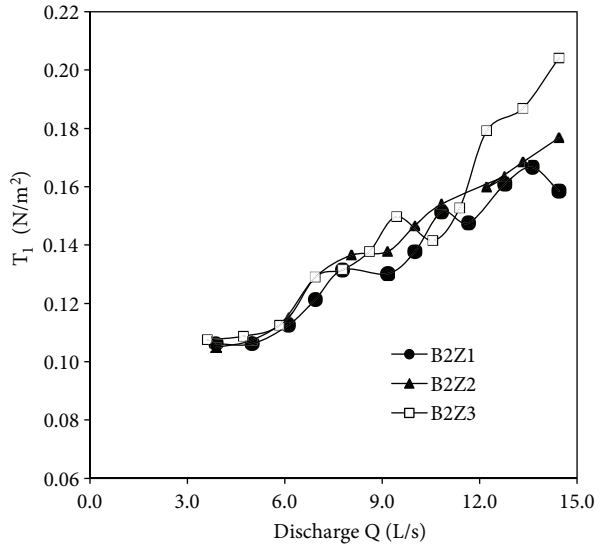

Figure 4. Average shear stress at the bottom of the main channel versus discharge for the models of constant step channel width (B = 15 cm).

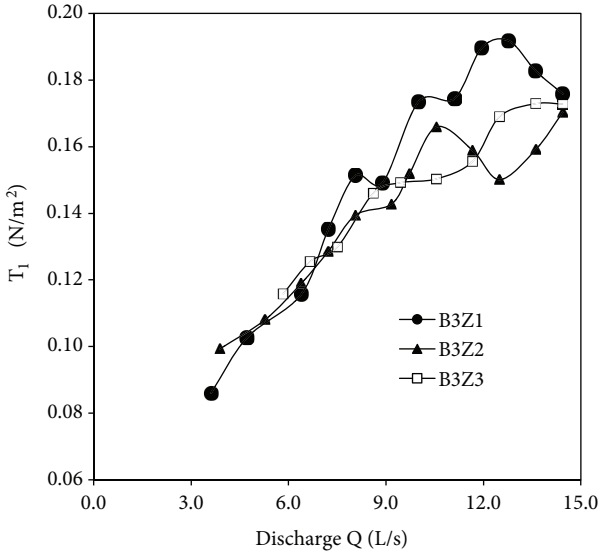

Figure 5. Average shear stress at the bottom of the main channel versus discharge for the models of constant step channel width (B = 20 cm).

3.2. Variation in T_1/T_5 with h/Z ratio

Some of the experimental results are shown in Figures 6–8 in the form of T_1/T_5 versus h/Z ratio. In order to see the effect of B and Z values on the T_1/T_5 ratio the figures were divided into two groups. In the first one the main channel width, B, was fixed and the step height, Z, was changed (Figures 6 and 7). Even though it is not possible to give a general conclusion about the variation of T_1/T_5 for the whole range of h/Z tested, in

general one can say that T_1/T_5 ratio increases as Z values increase for a given h/Z. In addition, as the h/Z ratio increases, the T_1/T_5 ratio increases. The second group (Figure 8) presents the data of the models of constant step heights. As a general trend, it can be noted that as the main channel width value increases, the T_1/T_5 ratio decreases.

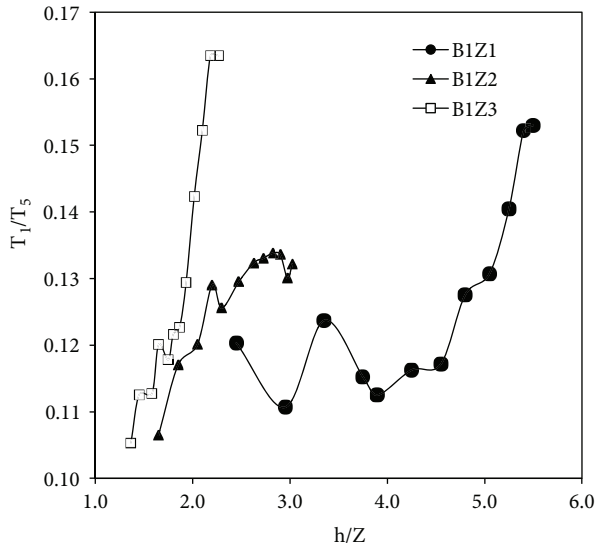

Figure 6. Comparison of T_1/T_5 ratios with h/Z ratio for the models of constant main channel width (B = 10 cm).

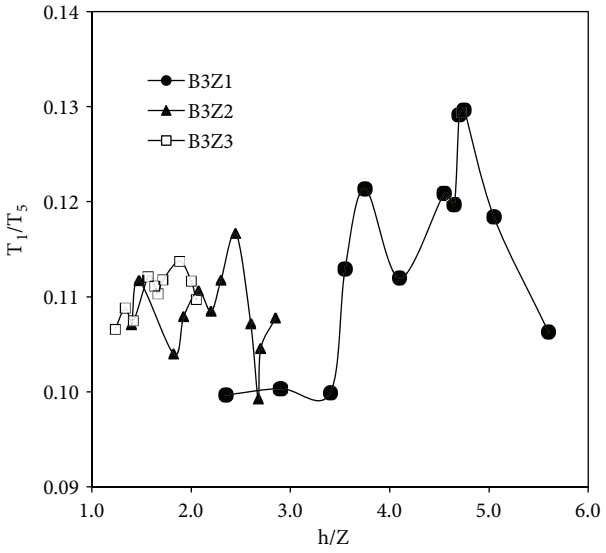

Figure 7. Comparison of T_1/T_5 ratios with h/Z ratio for the models of constant main channel width (B = 20 cm).

3.3. Variation in T_3/T_5 with h/Z ratio

The experimental results are shown in Figures 9–11 as T_3/T_5 versus h/Z. For some of the models tested T_3/T_5 ratio is directly affected by the geometry of the compound cross section. In order to see the effect of the channel

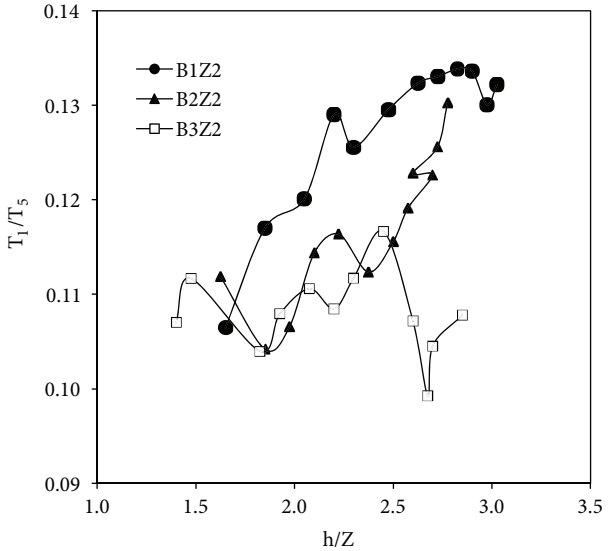

Figure 8. Comparison of T_1/T_5 ratios with h/Z ratio for the models of constant step height (Z = 4 cm).

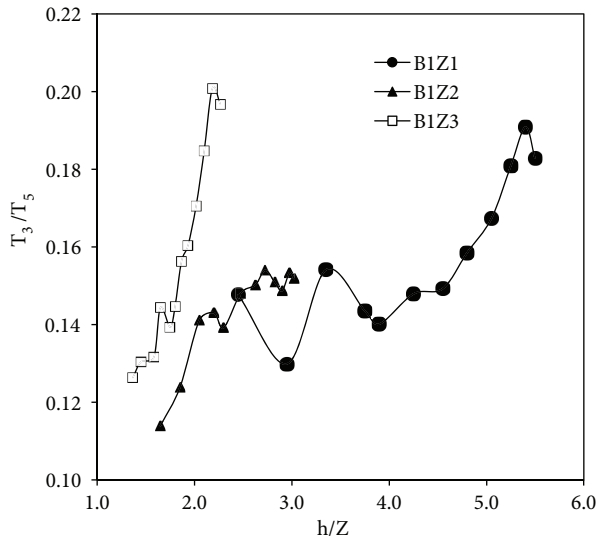

Figure 9. Variation in T_3/T_5 with h/Z ratio for the models of constant main channel width (B = 10 cm).

geometry on the T_3/T_5 versus h/Z, the figures were divided into two categories. The first one covers Figures 9 and 10, where B values were fixed while changing Z values. The figures show that the T_3/T_5 ratio increases as the h/Z ratio increases and reaches its maximum value of about 0.20 for model B1Z3. In addition, T_3/T_5 ratio increases as the Z value increases for a given h/Z ratio. On the other hand, Figure 11 is plotted to see the effect of varying B values on the T_3/T_5 ratio versus h/Z for constant Z values. This figure indicates that there is no clear effect of B values on T_3/T_5 ratio for a given h/Z value. The distribution of T_3/T_5 data on the figure for the whole range of h/Z tested is random; with increasing h/Z values, the ratio of T_3/T_5 might increase or decrease. Since flow in alluvial channels is influenced significantly by shear, it is obvious that the previous conclusion will be relevant in the analysis and design of such channels. The increases and decreases in shear stress will indicate the regions of possible erosion or deposition.

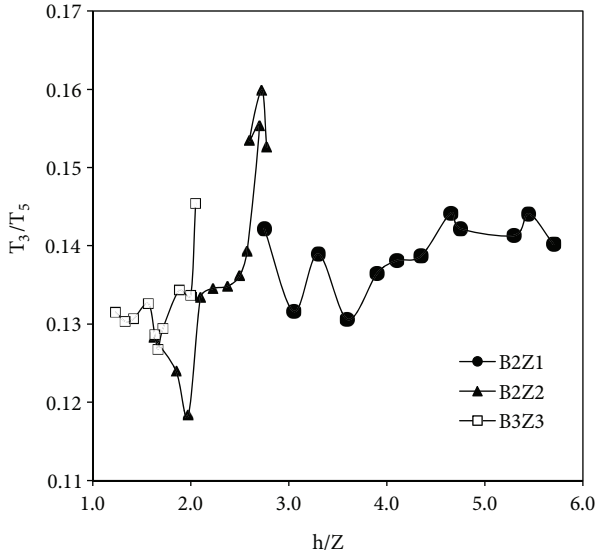

Figure 10. Variation in T_3/T_5 with h/Z ratio for the models of constant main channel width (B = 15 cm).

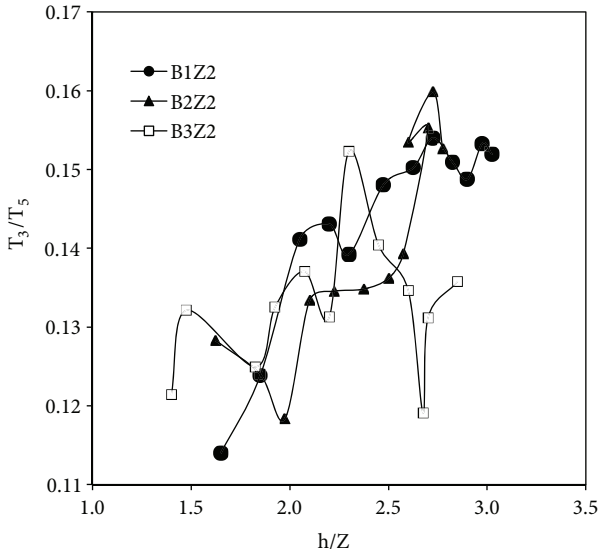

Figure 11. Variation in T_3/T_5 with h/Z ratio for the models of constant step height (Z = 4 cm).

3.4. Variation in T_3/T_1 with h/Z ratio and Y_f

The experimental results are shown in Figures 12–14 as T_3/T_1 versus h/Z ratio for some of the models tested. The h/Z ratio is directly affected by the geometry of the compound cross section. From these figures it can easily be seen that shear ratios are significantly affected at different depths with irregularities in the pattern and the occurrence of low and high ratios. Since the flow in alluvial channels is influenced significantly by shear, it is obvious that the previous conclusion will be relevant in the analysis and design of such channels. The decreases and increases in shear stress will indicate the regions of possible deposition and erosion [45].

In order to see the effect of channel geometry on the T_3/T_1 versus h/Z ratio the figures were divided into two categories. The first one covers Figure 12, in which B values were fixed while changing Z values. The figure shows that the T_3/T_1 ratio is mostly irregular for high Z values and reaches its maximum value of 1.33 in the model of B2Z3. On the other, hand Figures 13 and 14 are plotted to see the effect of varying B values on the T_3/T_1 ratio versus h/Z for constant Z values. For small Z value (Z = 2 cm), the figures indicate that as B values increase, the T_3/T_1 ratio increases for some of the given h/Z values and has no effect in the others

as the T_3/T_1 ratio values are randomly distributed. The values of T_3/T_1 varies between about 1.17 and 1.35 for the whole range of h/Z tested when the step height is equal to Z = 2 cm. For larger Z values (Z > 2 cm), it can be stated that as B value increases for a fixed Z value, T_3/T_1 increases for a given h/Z ratio.

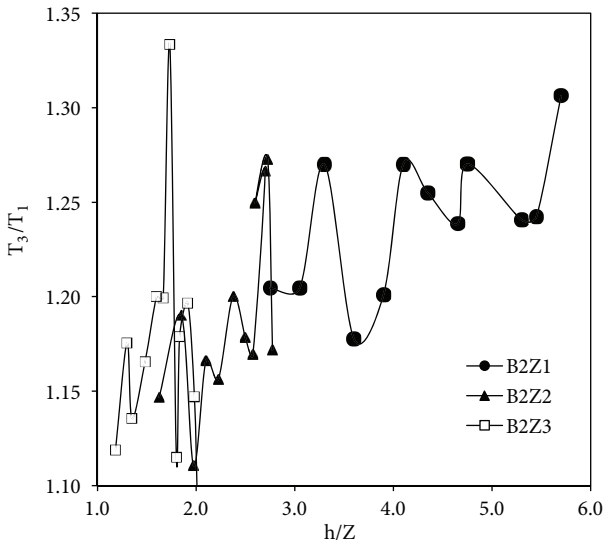

Figure 12. Variation in T_3/T_1 with h/Z ratio for the models of constant main channel width (B = 15 cm).

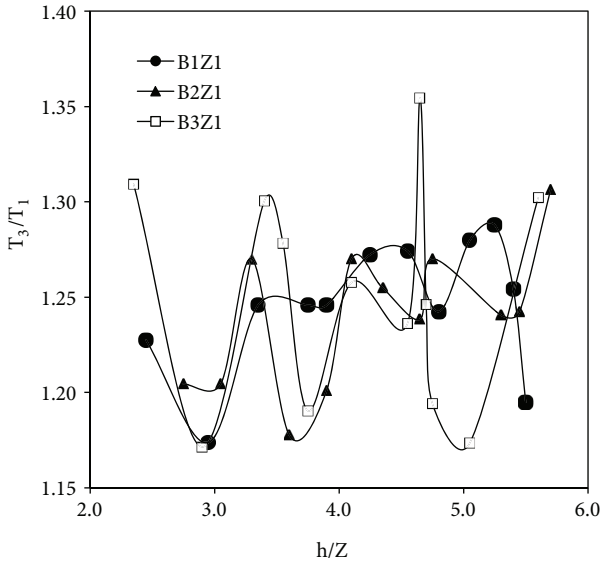

Figure 13. Variation in T_3/T_1 with h/Z ratio for the models of constant step height (Z = 2 cm).

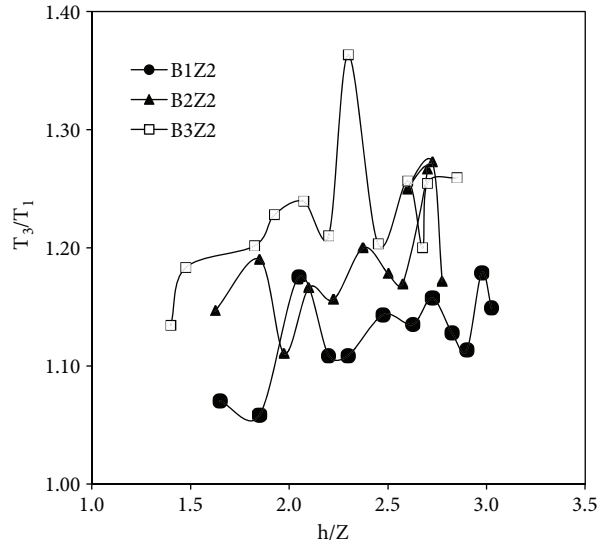

Figure 14. Variation in T_3/T_1 with h/Z ratio for the models of constant step height (Z = 4 cm).

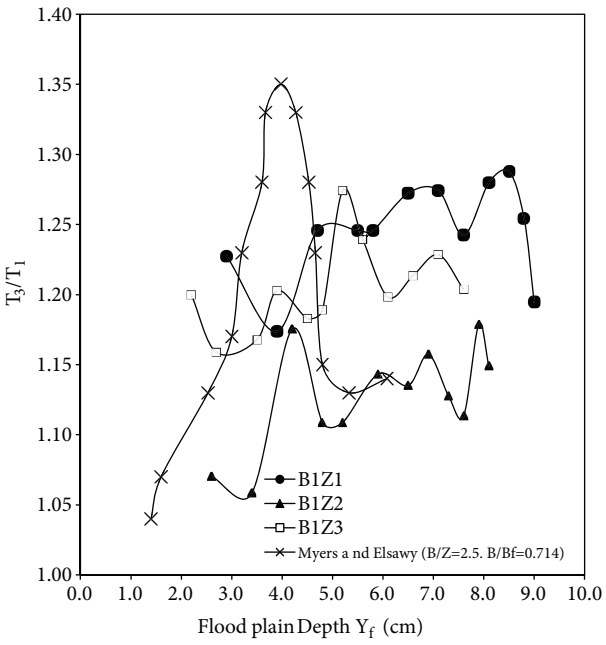

Figure 15. Comparison of T_3/T_1 versus Y_f of present results with those of Myers and Elsawy [25].

Variation in T_3/T_1 with floodplain depth, Y_f, is shown in Figure 15. It will be of importance, however, to compare the experimental results with those of Myers and Elsawy [25]. Their work was carried out in an asymmetric compound channel consisting of a deep section 25.4 cm wide by 10.16 cm deep and one floodplain of 35.56 cm wide by 7.62 cm deep giving a total depth of 17.78 cm. Of particular interest is a comparison of shear ratios of this compound channel and those of the models B1ZI (I = 1, 2, 3). The data of model B1Z2 and those of Myers and Elsawy follow almost the same path; since these models are geometrically very similar to each other, considering B/Z ratio, one can talk about the consistency between the experimentally obtained data.

3.5. Variation in T_2/T_6 with h/Z ratio

Some of the experimental results are shown in Figures 16–18 in the form of T_2/T_6 versus h/Z. In order to see the effect of channel geometry on the T_2/T_6 ratio with h/Z, the figures are divided into two groups. The first group consists of Figure 16 in which the effect of step height, Z, on the values of T_2/T_6 for models of constant main channel width is searched for. The T_2/T_6 ratio increases with increasing Z for a given h/Z value. For three different main channel widths, the step height of Z3 gives the maximum value of T_2/T_6. The second group of figures, including Figures 17 and 18, shows the effect of varying B values on the T_2/T_6 ratio with h/Z for constant Z values. It is clearly seen from Figure 16 with the smallest Z value (Z = 2 cm) that for a given h/Z, the T_2/T_6 ratio is the largest for the B value (B = 20 cm), but for large Z values (Z = 6 cm), the T_2/T_6 ratio increases as the B value increases for a given h/Z as shown in Figure 18. Eventually we can conclude that B3ZI models (I = 1, 2, 3) give the maximum T_2/T_6 ratio for a wide range of h/Z values investigated. We can also conclude from the related figures that T_2/T_6 is always less than 1.0. The reduction in the main channel shear stress is due to the presence of the interaction mechanism between the main channel and floodplains. This has the effect of reducing shear values due to the momentum transfer from the main channel to the floodplains. This effect is seen in all the figures related to the compound cross sections, where the T_2/T_6 ratio is always less than unity.

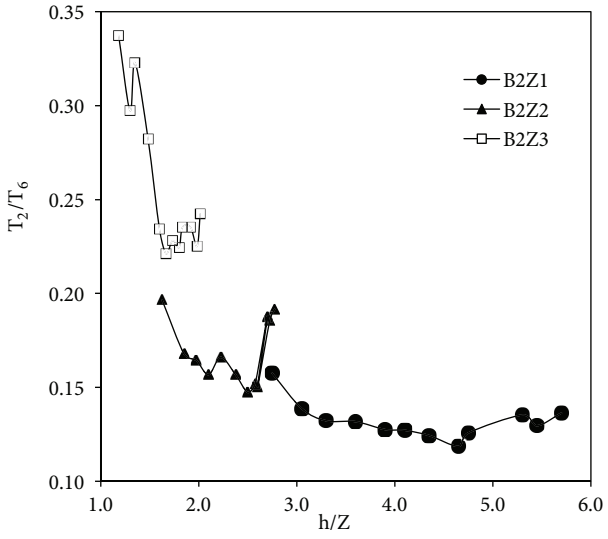

Figure 16. Variation in T_2/T_6 with h/Z ratio for the models of constant main channel width (B = 15 cm).

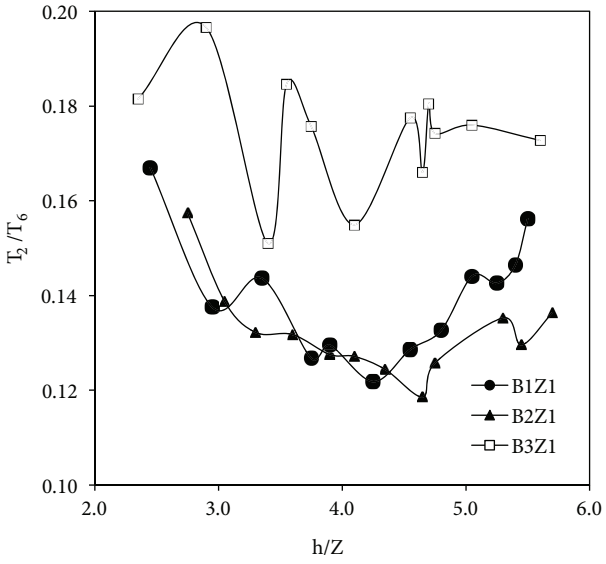

Figure 17. Variation in T_2/T_6 with h/Z ratio for the models of constant step height (Z = 2 cm).

3.6. Variation in T_4/T_6 with h/Z ratio

It is known from studies related to channels with loose boundaries that a ratio of significant importance is that of the maximum shear stress for any element of a cross section to the average cross sectional shear stress. This ratio is an indication of the uniformity of shear distribution and it is significant in alluvial channels to state the possible locations of erosion and deposition. Figures 19 and 20 show the variation in the ratios of the maximum floodplain bottom shear stress to the average floodplain cross sectional shear stress with h/Z ratio for constant main channel widths (B = 10 cm) and constant step heights (Z = 4 cm), respectively.

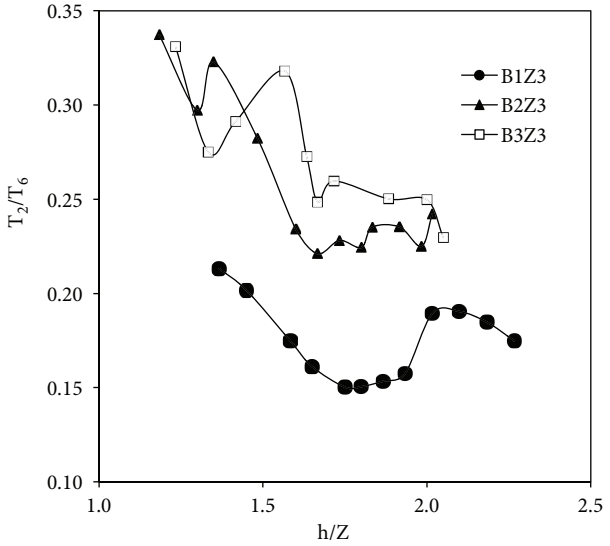

Figure 18. Variation in T_2/T_6 with h/Z ratio for the models of constant step height (Z = 6 cm).

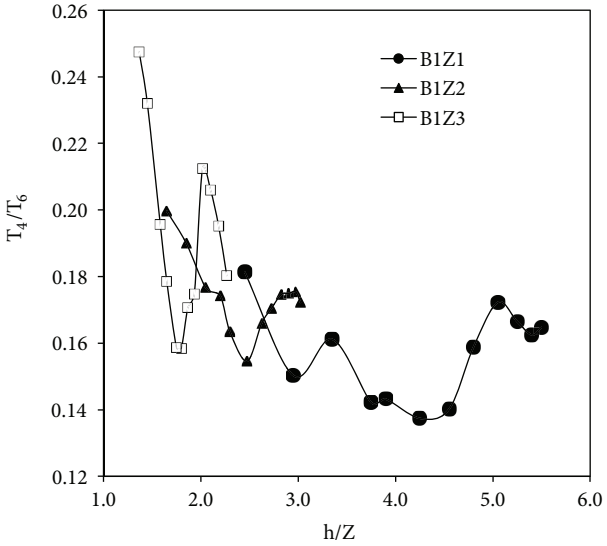

Figure 19. Variation in T_4/T_6 with h/Z ratio for the models of constant main channel width (B = 10 cm).

From the related figures it can be pointed out that T_4/T_6 ratio is almost regular for small step heights (Z = 2 and 4 cm) and large h/Z values and it becomes irregular for larger step heights and smaller h/Z values. Figure 20 reveals that as the main channel width increases, T_4/T_6 ratio increases for a given h/Z value. From the above-mentioned figures it can be concluded that the interaction between the main channel and floodplains has the effect of decreasing the shear ratios at high depths while increasing them randomly at lower depths.

3.7. Variation in T_4/T_2 with h/Z ratio and Y_f

Information regarding the nature of the floodplain boundary shear stress distribution in a compound channel flow is important to solve a variety of engineering and river hydraulics problems such as to give a basic understanding of the resistance relationship, to understand the mechanism of sediment transport, and to design stable channels and revetments. The variation in T_4/T_2 with h/Z ratio is shown in Figures 21 and 22 for models with constant main channel width and step height, respectively. The wall shear stress was integrated numerically over the bed of the floodplain, and an average value of the shear stress at the floodplain for each set of data and the ratio of T_4/T_2 was calculated and plotted against h/Z ratio. As can be seen from Figures 21 and 22, the presence of an interaction introduces irregularities in the distribution of the related data. As can be seen from Figure 21, there is no clear effect of step height on the T_4/T_2 ratio, but, from Figure 22, it is clear that the main channel width has an effect on this ratio and as the width of the main channel increases T_4/T_2 ratio increases.

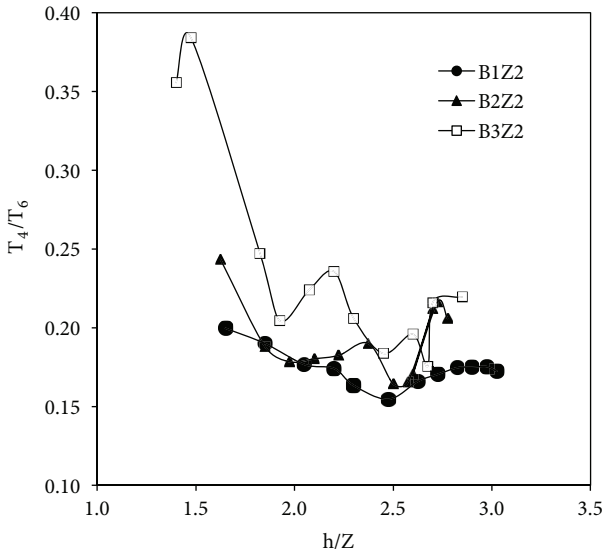

Figure 20. Variation in T_4/T_6 with h/Z ratio for the models of constant step height (Z = 4 cm).

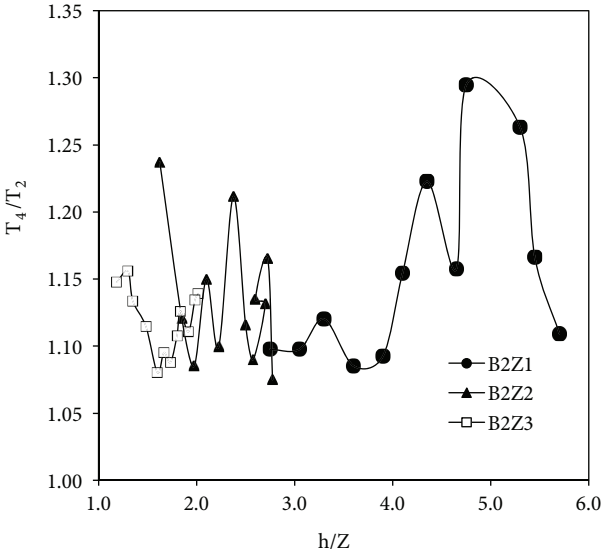

Figure 21. Comparison of T_4/T_2 ratios with h/Z ratio for the models of constant main channel width (B = 15 cm).

Variation in T_4/T_2 with floodplain depth, Y_f, is shown in Figure 23. Again, a comparison is made between the data of the present study and those of Myers and Elsawy [25] mentioned in the previous subsection as shown in Figure 23. The data of model B1Z2 and those of Myers and Elsawy follow almost the same path; since these models are geometrically very similar to each other, considering B/Z ratio (which equals 2.5 for both), one can talk about the consistency between experimentally obtained data.

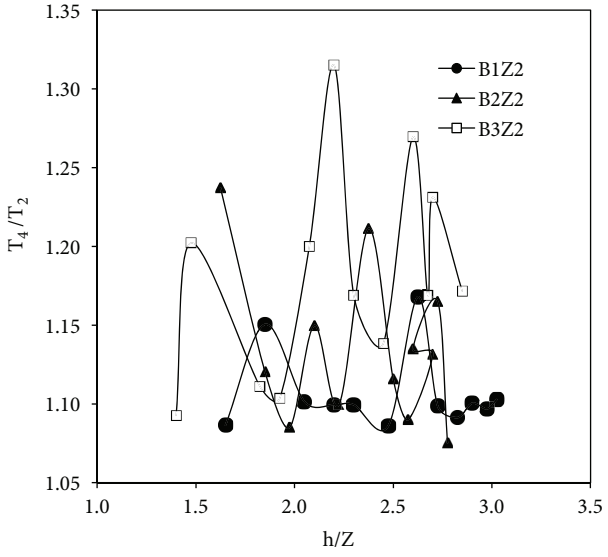

Figure 22. Comparison of T_4/T_2 ratios with h/Z ratio for the models of constant step height (Z = 4 cm).

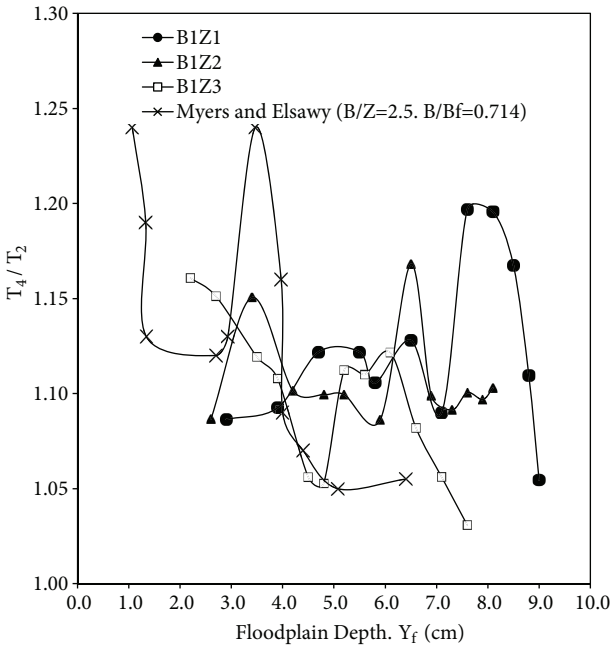

Figure 23. Comparison of T_4/T_2 versus Y_f of the present results with those of Myers and Elsawy [25].

4. Conclusions

The distribution of boundary shear stress along the bed of the main channel and floodplain perimeter of nine asymmetrical straight rectangular compound channel models has been presented. The geometry effect on the shear stress distribution in the main channel and floodplains due to the momentum transfer between the main channel section and floodplains has been investigated. From the analysis of the experimental results the following conclusions are drawn:

1. With the increase in floodplain width in the models of constant step height, as B_f increases, T_1 values decreases, and in the channels of constant floodplain width, if Z values increase, T_1 values increase.

2. For a fixed B value, T_1/T_5 ratio increases as Z values increase for a given h/Z. In addition, as the main channel width value increases T_1/T_5 ratio decreases for a given h/Z and a fixed Z value.

3. T_3/T_5 ratio increases as Z value increases for a given h/Z ratio and there is no clear effect of B values on the T_3/T_5 ratio for a given h/Z value and fixed Z value.

4. T_3/T_1 ratio is mostly irregular for high Z values and reaches its maximum value of 1.33 in the model of B2Z3. For larger Z values (Z $>$ 2 cm), as B value increases for a fixed Z value, T_3/T_1 increases for a given h/Z ratio.

5. The T_2/T_6 ratio increases with increasing Z for a given h/Z value. The T_2/T_6 ratio increases as the B value increases for a given h/Z. B3ZI models (I = 1, 2, 3) give the maximum T_2/T_6 ratio for most of the h/Z values investigated and T_2/T_6 is always less than 1.0.

6. As the main channel width increases, the T_4/T_6 ratio increases for fixed Z and a given h/Z value for most of the h/Z values tested.

7. There is no clear effect of step height on the T_4/T_2 ratio for constant B, but main channel width has an effect on this ratio, and as the width of the main channel increases the T_4/T_2 ratio increases for a given h/Z ratio.

8. The findings of this study can be used in equations of bed loads in which the relationships for shear stresses at the channel bottoms are required in addition to critical shear stresses as a function of soil type, through these kinds of channels.

Nomenclature

The following symbols are used in this paper:

A_f	area of the floodplain.
A_{mc}	the area of the main channel.
B	bottom width of the main channel.
B_f	floodplain width.
B_O	bottom width of the upstream channel.
d	probe outside diameter.
g	gravitational acceleration.
h	total water depth of compound cross section.
Y_f	floodplain water depth.
P_f	wetted perimeter of the floodplain.
P_{mc}	wetted perimeter of the main channel.
Q	volume rate of flow.
R_f	hydraulic radius of the floodplain.
R_{mc}	hydraulic radius of the main channel.
Z	depth of the main channel (step height).
ΔP	Preston tube pressure difference.
γ	fluid specific weight.
ρ	fluid density.
ν	the kinematic viscosity of the fluid.
τ_o	boundary shear stress.
S_o	energy slope.
X^*	the log of dimensionless differential pressure.
Y^*	the log of dimensionless shear stress.

Y_f	floodplain water depth.
T_k	measured shear stress at the kth point.
T_1	average shear stress at the bottom of main channel.
T_2	average shear stress at the bed of floodplains.
T_3	maximum shear stress at the bottom of main channel.
T_4	maximum shear stress at the bed of floodplains.
T_5	mean shear stress at the bottom of the main channel and equals $\gamma R_{mc} S_0$.
T_6	mean shear stress at the bed of the floodplain and equals $\gamma R_f S_0$.
U_∞	free stream velocity.
U(y)	mean velocity profile.
y	normal distance from the wall.

References

[1] Tominaga A, Nezu I, Ezaki K, Nakagawa H. Three dimensional turbulent structure in straight open channel flows. J Hydraul Res 1989; 27: 149–173.

[2] Zheng Y, Jin YC. Boundary shear in rectangular ducts and channels. J Hydraul Eng 1998; 124: 86–89.

[3] Rameshwaran, P, Naden PS. Three-dimensional numerical simulation of compound channel flows. J Hydraul Eng 2003; 129: 645–652.

[4] Yang SQ, McCorquodale JA. Determination of boundary shear stress and Reynolds shear stress in smooth rectangular channel flows. J Hydraul Eng 2004; 130: 458–462.

[5] Zarrati AR, Jin YC, Karimpour S. Semi-analytical model for shear stress distribution in simple and compound open channels. J Hydraul Eng 2008; 134: 205–215.

[6] Guo J, Julien PY. Turbulent velocity profiles in sediment laden flows. J Hydraul Res 2001; 39: 11–23.

[7] Babaeyan-Koopaei K, Ervine DA, Carling PA, and Cao Z. Velocity and turbulence measurements for two overbank flow events in River Severn. J Hydraul Eng 2002; 128: 891–900.

[8] Guo J, Julien PY. Shear stress in smooth rectangular open-channel flows. J Hydraul Eng 2005; 131: 30–37.

[9] Julien PY. Erosion and Sedimentation. Cambridge, UK: Cambridge University Press; 1995.

[10] Cheng NS. Exponential formula for bedload transport. J Hydraul Eng 2002; 128: 942–946.

[11] Berlamont JE, Trouw K, Luyckx G. Shear stress distribution in partially filled pipes. J Hydraul Eng 2003; 129: 697–705.

[12] Bocchiola D, Menduni G, Ward D. Testing block probes for wall shear stress measurement in water flows. J Hydraul Eng 2003; 129: 102–109.

[13] Cheng N, Sumer BM, FredsØe J. Investigation of bed shear stresses subject to external turbulence. International Journal of Heat and Fluid Flow 2003; 24: 816–824.

[14] Eckelmann H. The structure of the viscous sublayer and the adjacent wall region in a turbulent channel flow. J Fluid Mech 1974; 65: 439–459.

[15] Wietrzak A, Lueptow RM. Wall shear stress and velocity in a turbulent axisymmetric boundary layer. J Fluid Mech 1994; 259: 191–218.

[16] Colella KJ, Keith WL. Measurements of wall shear stress fluctuations beneath a turbulent boundary layer, 1997, In: Turbulent Flows, The 1997 ASME Fluids Engineering Division Summer Meeting, vol. 1. American Society of Mechanical Engineers, Fluids Engineering Division (Publication) FED, New York, USA, 1997; pp. 1–5.

[17] Chew YT, Khoo BC, Lim PC, Teo CJ. Dynamic response of a hot-wire anemometer. Part II: A flush-mounted hot wire and hot-film probes for wall shear stress measurements. Meas Sci Technol 1998; 9: 764–778.

[18] Miyagi N, Kimura M, Shoji H, Saima A, Ho CM, Tung S, Tai YC. Statistical analysis on wall shear stress of turbulent boundary layer in a channel flow using micro-shear stress imager. Int J Heat Fluid Flow 2000; 21: 576–581.

[19] Blinco PH, Simons DB. Characteristics of turbulent boundary shear stress. J Eng Mech Div ASCE 1974; 100: 203–220.

[20] Obi S, Inoue K, Furukawa T, Masuda S. Experimental study on the statistics of wall shear stress in turbulent channel flows. Int J Heat Fluid Flow 1996; 17: 187–192.

[21] Thomas WA, Prashum AI. Mathematical model of scour and deposition. J Hydr Div 1977; 110: 1613–1641.

[22] Holly FM, Rahuel JL. New numerical/ physical framework for mobile-bed modeling, part 1: numerical and physical principles. J Hydraul Res 1990; 28, 401–416.

[23] Lee HY, Hsieh HM, Yang JC, Yang CT. Quasi-two-dimensional simulation of scour and deposition in alluvial channels. J Hydraul Eng 1997; 123: 600–609.

[24] Paquier A, Khodashenas S. River bed deformation calculated from boundary shear stress. J Hydraul Res 2002; 40: 603–609.

[25] Myers WRC, Elsawy EM. Boundary shear in channels with floodplain. J Hydr Div 1975; 101: 993–1025.

[26] Lai CJ. Flow resistance, discharge capacity and momentum transfer in smooth compound closed ducts. PhD, University of Birmingham, UK, 1986.

[27] Lai CJ, Knight DW Distributions of streamwise velocity and boundary shear stress in compound ducts, Proc. 3rd Int. Symp. on Rened Flow Modelling and Turbulence Measurements, IAHR, Ed. Iwasa Y, Tamai N, Wada A. Tokyo, Japan, 1988.

[28] Myers WRC, Brennan EK. Flow resistance in compound channels. J Hydraul Res IAHR 1990; 28: 141–155.

[29] Rhodes DG, Lamb EJ, Chance RJ, Jones BS. Automatic measurement of boundary shear stress and velocity distributions in duct flow. J Hydraul Res IAHR 1991; 29: 189–197.

[30] Rhodes DG, Knight DW. Distribution of shear force on the boundary of a smooth rectangular duct. J Hydraul Eng 1994; 120: 787–807.

[31] Knight DW, Cao S. Boundary shear in the vicinity of river banks. Proc Nat Conf Hydraulic Engrg ASCE 1994; Bualo, USA.

[32] Thornton CI, Abt SR, Morris CE, Fischenich JC. Calculating shear stress at channel-overbank interfaces in straight channels with vegetated floodplains. J Hydraul Eng 2000; 126: 929–936.

[33] Khatua KK, Patra KC. Boundary shear stress distribution in compound open channel flow. J Hydraul Res (ISH) 2007; 12: 39–55.

[34] Preston JH. The determination of turbulent skin friction by means of pitot tubes. J Royal Aeronautic Society 1954; 58: 109–121.

[35] Patel VC. Calibration of the Preston tube and limitations on its use in pressure gradients. J Fluid Mech 1965; 23: 185–208.

[36] Isaacs LT, Macintosh JC. Measurement of shear stress in open channels, Conf. on Hydraulics in Civ. Engrg., The Institution of Engineers, Sydney, Australia, pp. 115–119, 1990.

[37] Abaza KA, Al-Khatib IA. Generalization of shear stress distribution in rectangular compound channels. Turkish J Eng Env Sci 2003; 27: 409–421.

[38] Clauser FH. The turbulent boundary layer. Adv Appl Mech 1956; 4: 1–51.

[39] Wei T, Schmidt R, McMurtry P. Comment on the Clauser chart method for determining the friction velocity. Experiments in Fluids 2005; 38: 695–699.

[40] Knight DW, Macdonald JA. Hydraulic resistance of artificial strip roughness. J Hydr Div ASCE 1979; 105: 675–690.

[41] Knight DW. Boundary shear in smooth and rough channels. J Hydr Div ASCE 1981; 107: 839–851.

[42] Knight DW, Demetriou JD. Floodplain and main channel flow interaction. J Hydraul Eng 1983; 109: 1037–1092.

[43] Baird JI, Ervine DA. Resistance to flow in channels with overbank floodplain flow. Proceedings of the 1st International Conference on Channels and Control Structures, 1984.

[44] McKee PM, Elsawy EM, McKeogh EJ. A study of the hydraulic characteristics of open channels with flodplains, IAHR, Proceedings of the 21st Congress, Melbourme, Vol. 3, 1985.

[45] Al-Khatib IA, Dmadi NM. Boundary shear stress in rectangular compound channels. Turkish J Eng Env Sci 1999; 23: 9–18.